22 Polarization-Induced False Colours

22.1 Polarization-Dependent Colour Sensitivity and Colour-Dependent Polarization Sensitivity

Glas (1975, 1976, 1980) was the first, who has hypothesized that false colours could be induced in an insect visual system by polarized light. He proposed that the honeybee *Apis mellifera* may perceive the polarization of skylight not as a distinct entity, but rather as "polarizational false colours". In his model, all UV, blue and green photoreceptors are involved in the perception of polarization. Since, according to the model, the UV and blue receptors are polarization sensitive, their output signals depend on the degree and direction of linear polarization. Consequently, the model retina should perceive "polarization-induced false colours".

Glas (1975, 1976, 1980) suggested that bees perceive such false colours when they are looking at the sky, and the resulting false colour pattern, the symmetry axis of which is the solar-antisolar meridian, could be used for orientation. He tested this hypothesis in behavioural laboratory experiments, in which honeybees oriented under differently coloured linear polarizers. He observed that the spontaneous orientation of bees relative to the artificial overhead E-vector direction depended on colour. From these experiments he concluded that the observed changes in the distribution of the running directions of bees can only be understood by assuming that integration of the contributions of receptors with different spectral types occurs in polarization perception. Although later studies did not confirm several details of the anatomical and receptor physiological assumptions of this model, and the results of the mentioned behavioural experiments with bees could have been interpreted otherwise (see e.g. Wehner 1982, p. 121), the relevance of this model is obvious in the study of polarization-induced false colours.

Honeybees *Apis mellifera* respond to skylight polarization and use it for navigation. The polarization-sensitive UV photoreceptors concerned are gathered in an upward-pointing narrow dorsal rim area of the eye. Except for this specialized eye region, the retina of honeybees is composed of photoreceptors that are twisted about their longitudinal axes (Wehner et al. 1975), so that their polarization sensitivity is almost abolished (Labhart 1980). Lau (1976) observed that honeybees fail to discriminate polarization patterns that mark a food source,

i.e. are presented to the frontal part of their eyes. The reason for this is that the frontal part of the eye is polarization-blind due to rhabdomeric twist. Similar twisted photoreceptors, or receptors in which the microvilli of the rhabdomeres are not aligned consistently in a single particular direction, were found also in many other insects. In these photoreceptors the polarization sensitivity is weak, whereas the untwisted receptors located at the dorsal rim of the eye and used exclusively for detecting skylight polarization exhibit high polarization sensitivity.

Wehner and Bernard (1993) proposed that the functional significance of the photoreceptor twist is to avoid the "polarization-induced (or simply polarizational) false colours" of natural surfaces such as leaves and petals of flowers, which reflect partially linearly polarized light. The degree and angle of linear polarization of reflected light depend on how smooth the plant surfaces are and how they are oriented with respect to the incoming light at the direction of view. For a flower-visitor this could cause difficulties, because the absorbing photopigments responsible for colour vision are contained in receptors with different microvillar orientations. Thus, each receptor gives a signal that depends not only on intensity and wavelength but also on the angle and degree of polarization. If the sensors of a colour vision system are also polarization sensitive, the system generates false colours that may obscure the real colours defined by the spectral properties of the object.

As Wehner and Bernard (1993) pointed out: "... when zig-zagging over a meadow with all its differently inclined surfaces of leaves, the bee would experience pointillistic fireworks of false colors that would make it difficult to impossible to detect the real colors of the flowers". The twist of photoreceptors of the colour vision system abolishes the ability to respond selectively to the plane of polarization. This allows each type of receptor to take part unambiguously in the bee's trichromatic colour vision system. To demonstrate the false colour problem Wehner and Bernard (1993) computed the shift of perceived colour caused in the bee's colour triangle when it views reflections from a dandelion leaf at different angles.

Marshall (1988) suggested that each of rows 5 and 6 of the midband in the compound eyes of mantis shrimps may contain a separate three-channel polarization-analyzer system with output comparisons: In row 5 between retinula cells R8, R1-R2-R5-R6 and R3-R4-R7; in row 6 between R8, R1-R2-R5 and R3-R4-R6-R7, which receptor triplets have different microvilli directions. Since the spectral sensitivities of R8 and R1-R7 cells are maximal at 350 and 500 nm, respectively (Cronin and Marshall 2001), in both types of the three-channel polarization-sensitive system suggested by Marshall (1988) polarization-induced false colours would be inevitably generated. However, to prevent such confusion between polarization and spectral information, in the ommatidia specialized for colour vision the rhabdoms are polarization-insensitive due to randomly oriented microvilli (Marshall et al. 1991b).

Mammals represent an extrema in the solution of the problem of polarization-induced false colours: they eliminate polarizational false colours in such a way that they have colour vision but are polarization-blind. Certain cephalopod (squid, cuttlefish and octopus) species are the other extrema: they are colour-blind but

polarization sensitive (Hanlon and Messenger 1996). Hypotheses about salmon polarization sensitivity also predict an interaction between colour and polarization (Novales Flamarique et al. 1998). Ultraviolet-, green- and red-sensitive cones appear to contribute to both spectral and polarization sensitivity in several salmonid fishes (Parkyn and Hawryshyn 2000). Thus, also these fishes may perceive polarization-induced false colours. The counterpart of polarization-dependent colour vision, namely colour-dependent polarization sensitivity has been found in *Daphnia pulex* (Novales Flamarique and Browman 2000).

Horváth et al. (2002c) gave a quantitative model to calculate such polarizational false colours with the use of polarization patterns measured by imaging polarimetry. In this chapter some results obtained with this model are presented.

22.2 Polarizational False Colours of Leaves and Flowers Perceived by *Papilio* Butterflies

Kelber (1999) and Kelber et al. (2001) suggested that the butterflies *Papilio aegeus* and *Papilio xuthus* do not process polarization and colour separately, and thus they may perceive polarization-induced false colours due to their weakly polarization-sensitive photoreceptors. Since Kelber and collaborators worked with artificial stimuli having an unnaturally high degree of linear polarization $p = 100\%$ which is not characteristic for light reflected from plant surfaces, no published behavioural data so far support that there is a significant influence of polarization on butterfly colour vision under natural conditions, when the receptors are stimulated by partially linearly polarized light with frequently low p. Since the polarization sensitivity of photoreceptors in *Papilio* species, ranging between $PS = 1.3$ and 2 (Bandai et al. 1992; Kelber et al. 2001), is very low[1], the questions arise:

- Can the often low p of light reflected from plant surfaces induce sufficiently strong polarizational false colours in *Papilio* butterflies to influence their colour vision significantly?
- How do these polarization-induced false colours depend on the different parameters of the butterfly retina (microvillar directions, polarization sensitivity, orientation of the eye), on the characteristics of the optical stimuli (degree and angle of polarization of reflected light) and on the illumination conditions (alignment of the plant surface with respect to the direction of view and to the solar direction; plant surface in direct sunshine or in shadow)?

[1] Note that $PS = 1$ for polarization-insensitive receptors, and $PS = 1.3$-2 are such low values that many researchers consider a photoreceptor with such PS-values as polarization insensitive. Laughlin (1976, p. 227), for example, wrote about the polarization-insensitive photoreceptors of the dragonfly *Hemicordulia tau*: "All linked pigment cells and the single pigment green cells are notable for their lack of PS (< 2.5) at peak wavelength."

Shashar et al. (1998) investigated the polarization of light in a tropical rain forest and demonstrated some polarizational features of light reflected from certain leaves. Continuing the analysis done by Wehner and Bernard (1993), Horváth et al. (2002c) quantitatively estimated the influence of polarization sensitivity on the perception of natural surface colours by *Papilio* butterflies.

22.2.1 Computation of the Spectral Loci of Colours Perceived by a Polarization- and Colour-Sensitive Retina

The numerical values of the retina model of Horváth et al. (2002c) (Fig. 22.1) described in this chapter are characteristic to the butterfly *Papilio xuthus* (Fig. 1B and Table 1 of Kelber et al. 2001, pp. 2470-2471). The model retina contains polarization-sensitive photoreceptors of spectral types red (R), green (G) and blue (B), with sensitivity maxima at λ_R^r = 600 nm, λ_G^r = 520 nm and λ_B^r = 460 nm. The relative absorption functions of the receptors are shown in Fig. 22.1A. In the retina model, angle β is the direction of the microvilli measured clockwise from the dorso-ventral meridian of the compound eye (Fig. 22.1C). For the microvilli of the blue photoreceptors $\beta_B = 0^o$, in the green receptors $\beta_G = 0^o$, 35^o, 90^o, 145^o and in the red receptors $\beta_R = 0^o$, 35^o, 145^o (Fig. 22.1B). The colour vision system of *Papilio* butterflies is pentachromatic (Arikawa et al. 1987). Treating the short-wavelength receptors (UV, violet, blue) as one receptor type, allows to demonstrate false colour effects in a plausible way by indicating the shifts of colour loci in the equilateral colour triangle (Fig. 22.1E). No principally different false colour effects are expected by including all five receptor types in the retina model.

If the electric field vector E of totally linearly polarized incident light is parallel (par) to the longitudinal axes of the microvilli, a polarization-sensitive photoreceptor of type *r (=R,G,B)* absorbs P_r-times the number of photons (in the following called quantum absorption) as in the case when the E-vector is perpendicular (perp) to the microvilli. Thus, the relationship between the numbers of absorbed quanta is: $q_r^{par} = P_r q_r^{perp}$, where P_r is the polarization sensitivity ("*PS*-value") of the receptor, and q_r is the quantum absorption. The polarization sensitivity of the photoreceptors in *Papilio xuthus* ranges from 1.3 to 2 at peak wavelengths (Kelber et al. 2001, p. 2471, Table 1). In the retina model $P_B = P_G = P_R = 2$ are chosen, by which the average polarization sensitivity is slightly overestimated.

Let the angle of the eye's dorso-ventral meridian be χ clockwise from the vertical (Fig. 22.1C). If receptor r receives partially linearly polarized light with intensity $I(\lambda)$, degree of linear polarization $p(\lambda)$, angle of polarization $\alpha(\lambda)$ (clockwise from the vertical), minimum and maximum E-vectors $E_{min}(\lambda)$ and $E_{max}(\lambda)$, respectively, the quantum absorption q_r can be calculated as follows:

$$q_r = k \int_0^\infty A_r(\lambda) \left[P_r E^{par}{}_{max}(\lambda)^2 + E^{perp}{}_{max}(\lambda)^2 + P_r E^{par}{}_{min}(\lambda)^2 + E^{perp}{}_{min}(\lambda)^2\right] d\lambda, \qquad (22.1)$$

where k is a constant, λ is the wavelength of light, $A_r(\lambda)$ is the relative absorption of the receptor (Fig. 22.1A), $E^{par}{}_{max}(\lambda)$, $E^{perp}{}_{max}(\lambda)$ and $E^{par}{}_{min}(\lambda)$, $E^{perp}{}_{min}(\lambda)$ are the parallel and perpendicular components of the electric field vectors $E_{max}(\lambda)$ and $E_{min}(\lambda)$ with respect to the microvillar direction. From Fig. 22.1C one can read:

$$E^{par}{}_{max}(\lambda) = E_{max}(\lambda)\cos[\alpha(\lambda) - \chi - \beta_r], \quad E^{perp}{}_{max}(\lambda) = E_{max}(\lambda)\sin[\alpha(\lambda) - \chi - \beta_r],$$

$$E^{par}{}_{min}(\lambda) = -E_{min}(\lambda)\sin[\alpha(\lambda) - \chi - \beta_r], \quad E^{perp}{}_{min}(\lambda) = E_{min}(\lambda)\cos[\alpha(\lambda) - \chi - \beta_r]. \tag{22.2}$$

The relationship between $E^2{}_{min}(\lambda)$, $E^2{}_{max}(\lambda)$ and $p(\lambda)$ is:

$$E^2{}_{min}(\lambda) = E^2{}_{max}(\lambda)\,[1-p(\lambda)]/[1+p(\lambda)]. \tag{22.3}$$

The intensity $I(\lambda)$ can be expressed with $E_{min}(\lambda)$ and $E_{max}(\lambda)$ as follows:

$$I(\lambda) = k'\,[E^2{}_{max}(\lambda) + E^2{}_{min}(\lambda)]/2 = k'\,E^2{}_{max}(\lambda)/[1+p(\lambda)], \quad k' = \text{constant}. \tag{22.4}$$

Using Eqns. (22.1)-(22.4), one can obtain:

$$q_r = k''\int_0^{\infty} A_r(\lambda)\, I(\lambda)\, \{P_r[1+p(\lambda)] + 1 - p(\lambda) - 2p(\lambda)(P_r-1)\sin^2[\alpha(\lambda) - \chi - \beta_r]\}\,d\lambda,$$

$$r = R, G, B; \quad k'' = \text{constant}. \tag{22.5}$$

The expressions for k, k' and k'' involve different electrodynamical constants. Using them, one could calculate the absolute value of the absorbed quantum absorption q_r. We omit to give the expressions of k, k' and k'', because they all are eliminated in the final expressions describing the spectral loci of colours perceived by a polarization- and colour-sensitive retina.

Since using video polarimetry (Horváth and Varjú 1997), one can measure the spatial distribution of I, p and α of light reflected from plant surfaces only at wavelengths $\lambda_B{}^c = 450$ nm, $\lambda_G{}^c = 550$ nm and $\lambda_R{}^c = 650$ nm, in the calculations the following approximations are taken (Fig. 22.1D):

$$f(400\text{ nm} \le \lambda \le 500\text{ nm}) = f(\lambda_B{}^c) = f_{blue},$$

$$f(500\text{ nm} < \lambda < 600\text{ nm}) = f(\lambda_G{}^c) = f_{green},$$

$$f(600\text{ nm} \le \lambda \le 700\text{ nm}) = f(\lambda_R{}^c) = f_{red}, \qquad f = I, p, \alpha, \tag{22.6}$$

that is, in the spectral range s = red, green, blue the values of I, p and α are considered to be constant. This approximation can be applied, because the maxima and half bandwidths of the red, green and blue relative sensitivity functions of the camera of the used imaging polarimeter fall close to those of the corresponding

red, green and blue relative absorption functions $A(\lambda)$ (Fig. 22.1A) of the butterfly retina modelled. Then:

$$q_r = k'' \Sigma_s I_s[P_r(1+p_s) + 1 - p_s - 2p_s(P_r-1)\sin^2(\alpha_s - \chi - \beta_r)] \int_{\lambda s1}^{\lambda s2} A_r(\lambda)d\lambda,$$

$$r = R, G, B; \quad s = \text{red, green, blue;}$$

$$\lambda_{blue1} = 400 \text{ nm}, \quad \lambda_{blue2} = \lambda_{green1} = 500 \text{ nm},$$

$$\lambda_{green2} = \lambda_{red1} = 600 \text{ nm}, \quad \lambda_{red2} = 700 \text{ nm}. \tag{22.7}$$

In the literature of colour vision, there are two different conventions to give the relative absorption functions $A(\lambda)$ of photoreceptors: they possess either (i) equal amplitude $A_{max}(\lambda) = 1$ (e.g. Przyrembel et al. 1995; Fig. 12, p. 584), or equal integrals $\int_0^\infty A(\lambda)d\lambda = 1$ (e.g. Lunau and Maier 1995; Fig. 1A, p. 3). Kelber et al. (2001), for example, used the first convention, as Fig. 22.1A gives also the $A(\lambda)$ curves with the same amplitudes. This convention is called "amplitude normalization". The second convention, called "integral normalization", corresponds to the assumption that the quantum absorptions of receptors of different spectral types are the same if the incident light is unpolarized [$p(\lambda) = 0$] and physically white [$I(\lambda)$ = constant]. This has the consequence that "physical (or optical) white" coincides with "physiological (or perceptional) white"; in other words, the locus of both physical and physiological white is positioned at the colourless centre of the equilateral colour triangle of a colour vision system (Fig. 22.1E). In this case the receptor absorption curves are normalized by setting their integral to 1, that is, the quantum absorption q_r of receptor type r is divided by the quantum absorption

$$q_r^{white} = k'' I_{white} (P_r + 1) \Sigma_s \int_{\lambda s1}^{\lambda s2} A_r(\lambda)d\lambda \tag{22.8}$$

of the receptor for unpolarized ($p_s = 0$) and physically white light ($I_s = I_{white}$ = arbitrary constant). Then, the normalized quantum absorption is:

$$m_r = q_r/q_r^{white} = \{k''\Sigma_s I_s [P_r(1+p_s)+1-p_s-2p_s(P_r-1)\sin^2(\alpha_s-\chi-\beta_r)] \int_{\lambda s1}^{\lambda s2} A_r(\lambda)d\lambda\}/$$

$$/[k'' I_{white}(P_r+1) \Sigma_s \int_{\lambda s1}^{\lambda s2} A_r(\lambda)d\lambda]. \tag{22.9}$$

The three coordinates of the spectral locus of the perceived colour within an equilateral colour triangle (Fig. 22.1E) are

$$M_R = q_R/(q_R+q_G+q_B), \quad M_G = q_G/(q_R+q_G+q_B), \quad M_B = q_B/(q_R+q_G+q_B) \tag{22.10}$$

for amplitude normalization, and

$$M_R = m_R/(m_R+m_G+m_B), \quad M_G = m_G/(m_R+m_G+m_B), \quad M_B = m_B/(m_R+m_G+m_B) \qquad (22.11)$$

for integral normalization. Note that the constants k'' and I_{white} are eliminated from the expressions of M_R, M_G and M_B, as mentioned above. The calculations were performed for both amplitude and integral normalizations, but both conventions provided very similar results. The only significant difference between them is that for integral normalization the colour loci remain close to the white point (centre of the colour triangle), i.e. the colours are extremely pale, while for amplitude normalization all colour loci slightly shift towards the red-green border of the colour triangle. The reason for the latter shift is that the integral of $A_G(\lambda)$ is the greatest among the integrals of the absorption curves of the red, green and blue receptors (see Fig. 22.1A). Hence, when amplitude normalization is used, the quantum absorption q_G of the green receptors is the largest resulting in that the component M_G will be the greatest. If integral normalization is used, the relative differences in the quantum absorptions q_R, q_G and q_B of the R, G and B receptors are reduced, which decreases the colour saturation. In this chapter only the results are presented that were obtained using the more common integral normalization, which puts white in the intuitively correct location in the middle of the colour triangle. The values of I_s, p_s and α_s originate from the reflection-polarization patterns measured by imaging polarimetry in the s = red, green, blue ranges of the spectrum.

Using Eqns. (22.10) and (22.11), the coordinates M_r (r=R,G,B) of the colour locus are computed for every pixel of a given picture of plant surfaces. The calculated spectral coordinates M_r are plotted within the equilateral colour triangle (Fig. 22.1E). Note that the peak wavelengths of the colour receptors in the human eye differ significantly from those of the *Papilio* retina. Thus the false colour pictures given in this chapter merely serve to visualize the effect of polarization-induced colour changes for the reader. The false colours will look differently to a butterfly.

22.2.2 Polarization-Induced False Colours Perceived by the Polarization- and Colour-Sensitive Model Retina

Figure 22.2 shows the reflection-polarizational characteristics of the red flower petals and green leaves of *Campsis radicans* (trumpet vine, Bigniniaceae). In Fig. 22.3A the colours of *Campsis radicans* are shown as perceived by a polarization-blind retina. They are considered as "real" colours and serve as reference: the shifts of the polarization-induced false colour loci in the colour triangle are measured from the loci of these real colours. Figures 22.3B-E show the false colours of the plant perceived by the weakly polarization-sensitive retina of *Papilio xuthus* as a function of the alignment χ of the dorso-ventral symmetry plane of the eye with respect to the vertical, when a given set of photoreceptors rotates in front of the plant. Rotating the polarization-sensitive receptor set by 180^o, the perceived false colours shift continuously in the colour triangle passing within an approximately elliptical chromatic area: in cases B, C, D and E of Fig.

22.3 the false colour of the leaves, for example, is slightly blue-greenish, bluish, reddish and greenish, respectively. These colours are, however, more or less masked by the whitish reflected light (see Fig. 22.2A). Similar shifts of the perceived colour occur if the relative position of the plant surface with respect to the receptor set (orientation of the dorso-ventral meridian of the eye) changes because of rotation and/or translation. In the case of *Papilio xuthus* the chromatic distances of the polarization-induced false colours from the real colour are small due to the relatively small *PS*-value of 2 of the retina. These chromatic distances are smaller for the matt petals reflecting light with lower p than for the shiny leaves reflecting light with much higher p.

Figure 22.3 also demonstrates how the real and the polarization-induced false colours of leaves depend on the orientation of leaf blades. Although the average alignment of leaf blades is approximately horizontal, there are considerable deviations from this direction (see Fig. 22.2A; the E-vector alignment of specularly reflected light is always perpendicular to the plane of reflection determined by the incident ray, reflected ray and the normal vector of the reflecting surface). The more or less randomly curved leaf blades are more or less randomly oriented around the horizontal direction, thus both p and α change from site to site. The consequence is that the homogeneously green real colour of the leaves being independent of p and α (see the narrow colour distribution around the most frequent real green colour of leaves in the right colour triangle of Fig. 22.3A of the leaves) becomes more heterogeneous for a polarization-sensitive retina resulting in different colour hues ranging from (although partly white-masked) violet through blue, green, yellow, orange to red (see the relatively wide false colour distribution around the most frequent green false colour of leaves in the colour triangles of Figs. 22.3B-E). This shows one of the consequences of the polarization sensitivity of colour vision: due to the high diversity of p and α of light reflected from plant surfaces, the perceived polarizational false colours are more diverse than the real colours. This phenomenon makes more difficult to recognize a given real colour and demonstrates a disadvantage of the perception of polarization-induced false colours.

In *Papilio xuthus*, the microvilli in the red and green receptors can have three or four different directions as given in Fig. 22.1B, and at present it is not known how the receptors contribute to the net neural polarizational signal. It is only known that in the blue receptors the microvillar direction is $\beta_B = 0^o$. Apart from the contribution of $\beta_R = 145^o$, $\beta_G = 35^o$ and $\beta_B = 0^o$ (Fig. 22.3), other possible combinations of β_R and β_G (together with $\beta_B = 0^o$) are also used. Figure 22.4D shows how the polarization-induced false colours of an *Epipremnum aureum* plant (golden pothos, Aracea) perceived by *Papilio xuthus* depend on β_R and β_G. In the foreground of the colour picture in Fig. 22.4A the inflorescence of *E. aureum* can be seen which possesses a large, shiny, petal-imitating red leaf called spathe, while the background is composed of the shiny green leaves of the plant. Figures 22.4B and 22.4C show the patterns of p and α of the plant measured at 450 nm.

Figure 22.4D demonstrates the chromatic diversity of the polarizational false colours versus the microvillar direction. Depending on β_G and β_R, all false colours

b-m perceived by *Papilio xuthus* shift slightly towards the red and/or green hues with respect to the real colour *a* possessing the largest blue component M_B. This is because (i) the light reflected from the investigated areas of the plant was approximately horizontally polarized (Fig. 22.4C), and (ii) the microvillar direction of the blue receptor is dorso-ventrally (vertically) fixed. The false colours are scattered within areas, the dimensions of which are similar for both the spathe and the leaf, because both are shiny and reflect strongly polarized light (Fig. 22.4B).

Having based the previous considerations on a low polarization sensitivity of $PS = 2$, let us now consider visual systems with high PS. Figure 22.5 shows the dependence of the polarization-induced false colours on $P_B = P_G = P_R = P$ as a function of β_G and β_R. When P increases from 1 to 20, all false colours shift to some degree from the real unsaturated, bluish-green colour (locus *a*) of the leaf towards relatively saturated red, orange, yellow or green colours. The chromatic distance of the false colours from the real colour can be considerable if the polarization sensitivity is strong enough.

p of light reflected from plant surfaces depends on the angle of incidence, the surface roughness and the wavelength. At wavelengths, where the amount of light coming from the subsurface layers is negligible in comparison with the amount of light reflected from the surface, the reflected light can be almost totally polarized if the angle of incidence is near the Brewster angle (Horváth and Varjú 1997). This is the situation for shiny green leaves in the blue or red (Fig. 22.2), for instance. The increasing surface roughness decreases p. Hence, in nature p of light reflected from plant surfaces can vary between 0% and almost 100%. Figure 22.6 shows the dependence of the polarization-induced false colour on p of reflected light as functions of β_G and β_R. The dependence of the polarization-induced false colours on p (Fig. 22.6) is qualitatively the same as that on the polarization sensitivity P of the photoreceptors (Fig. 22.5). The only essential quantitative difference between Figs. 22.5 and 22.6 is that in the latter case the chromatic shifts (the lengths of the arrows) are much smaller than in the former case in spite of the very high p-values of 78%, 75%, 99% (Table 22.1).

Figure 22.7 shows how the spectral and reflection-polarizational characteristics of a sunlit leaf of a *Ficus benjamina* tree (weeping fig, Ficaceae) depend on the direction of sunlight at a given solar elevation, and how they change if the leaf is shaded from direct sunlight. The colours as well as p and α of light reflected from the leaf depend on the orientation of the leaf blade with respect to the sun. For a given position of the sun there are chromatic and polarizational differences between the sunlit and the shaded leaf. The colour of the sunlit leaf is always greenish (Figs. 22.7A,C,E,G) due to the diffuse scattering and selective absorption of white sunlight in the green subcuticular leaf tissue. This greenish hue is, however, more or less masked by strong specular reflection of white sunlight, if the leaf is viewed in the direction of the sun (Fig. 22.7G). The colour of the shaded leaf (Figs. 22.7B,D,F,H) is always bluish, because it is illuminated by blue skylight. Due to the non-planar curved shape of the leaf blade p and α of reflected light changes from point to point. In Fig. 22.7 the leaf blade in the small rectangular left and right window is approximately horizontal and vertical,

respectively. Note that although in Fig. 22.7G the entire leaf is lit by direct sunshine, both the left and right windows are placed in a local shaded region due to the curved leaf blade. Thus, both the left and right windows in case G represent a shaded situation.

In Fig. 22.8 we can see that under the clear blue sky the hues of shaded leaves are always nearer to the blue-green parts of the colour triangle than those of sunlit leaves. In the left window of the leaf in Fig. 22.7 the false colour shifts (represented by arrows) towards red, orange, yellow or green hues for both shaded and sunlit leaves. Since in the right window of the leaf in Fig. 22.7 the orientation of the leaf blade is different (vertical) from that (horizontal) in the left window, the colour shifts in the right window differ from those in the left window. Apart from case E, in the right window the false colours shift toward the green hues for both shaded and sunlit leaves. In case E the colour shift is very small.

22.2.3 Reflection-Polarizational Characteristics of Plant Surfaces

As we have seen above, the higher the p, the stronger is the colour shift, the direction of which depends on the viewing direction, the alignment of the dorso-ventral meridian of the eye, the polarization sensitivity, the microvillar orientation of the photoreceptors and the illumination conditions. Rough surfaces reflect light diffusely, which reduces polarization. Thus, the rougher a plant surface (e.g. due to a waxy layer or other microstructures), the lower the p of reflected light. The E-vector reflected from a plant surface follows its curvature, because the reflected light becomes partially linearly polarized perpendicularly to the plane of reflection for any dielectric reflector.

The darker a plant surface in a given spectral range, the higher the p of reflected light. The reason for this is the following: p of light reflected by the cuticle or epidermis of plants depends on the incident angle, but is almost independent of the wavelength. The direction of polarization of reflected light is parallel to the surface. The colour of plant surfaces arises from the selective absorption and diffuse scattering of light in the tissue below the transparent cuticle. The diffuse light emanating from this tissue is originally unpolarized, but it becomes partially polarized after transmission and refraction at the epidermis. The E-vector of the tissue-scattered light is perpendicular to the cuticle because of refraction polarization. Hence, the net degree and direction of polarization of a plant surface are determined by the superposition of the epidermis-reflected and the subcuticle-scattered light. If the former dominates (e.g. in sunlit shiny leaves observed from the direction of specular reflection), the direction of polarization is parallel to the cuticle; otherwise, the E-vector is perpendicular to it (e.g. sunlit leaves observed from behind, when the leaf-transmitted light is perceived). In those spectral regions where the subcuticle-scattered light has a considerable contribution, the net p of returned light is reduced or even abolished.

These general rules are demonstrated in Fig. 22.2: The considerably reduced amount of subcuticle-scattered light in the blue causes the red flowers to be dark and relatively strongly polarized at 450 and 550 nm. At 650 nm the amount of

light emanating from the red tissue below the epidermis of the flower is greater, thus, the net p is reduced. This is the physical reason for the general rule that in a given spectral region the darker objects polarize light to a higher degree if the illuminating light is unpolarized and white. Thus, green leaves are less polarized in the green than in the blue and the red, as can be well seen in Fig. 22.2.

Surfaces of petals have a matt finish, making them much better diffuse reflectors than leaves, which have a shiny, smooth cuticle (Kay et al. 1981). Thus, petals usually reflect diffuse and only weakly polarized light, while leaves reflect more specularly and the reflected light is generally highly polarized if the direction of view is near the Brewster angle.

Horváth et al. (2002c) proposed that the major function of the surface roughness of petals is not the reduction of p of reflected light (and thus the reduction of polarization-induced false colours), but to reduce the white glare of the surface, which would overwhelm the petal-tissue-backscattered coloured light and would make more difficult to perceive the real, attractive and striking colour of the petal. An appropriately rough petal surface functions as a Lambertian reflector, which reflects light uniformly in all directions independently of the angle of incidence. As a byproduct, the light reflected by a Lambertian surface is unpolarized. The intensity and colour of such a (matt) Lambertian surface is the same from all directions of view. If the surface of a petal were smooth, like the red spathe in Fig. 22.4A, it would function as a Fresnel reflector, which reflects light specularly. Then the intensity and colour of the petal-tissue-backscattered coloured light would be overwhelmed by the white glare (that is, by the specularly reflected white light) from the smooth cuticle if the direction of view coincides with the angle of reflection. This problem would not occur for other directions of view. Hence, the reduction of p of reflected light seems to be the consequence, and not the main aim of the surface roughness of petals. The roughness of petal surfaces is of great importance for all colour vision systems, independently of polarization-blindness or polarization-sensitivity, which must efficiently detect and distinguish the colours of flowers.

In columns 2 and 3 of Fig. 22.7, we can see that at a given illumination direction and in a given (e.g. blue) part of the spectrum the gross features of the patterns of p and α of the *Ficus* leaf are similar for both the sunlit and the shaded cases, although the colours of the sunlit and shaded leaf differ considerably. The reason for this is that the smooth *Ficus* leaf is similar to a Fresnel reflector, and the leaf blade is tilted so that sunlight cannot be reflected specularly from it towards the camera (apart from certain small curved areas). Thus, the sunlight reflected specularly from the leaf blade is not visible and does not add to the leaf-tissue-backscattered light. Large differences between the reflection-polarizational characteristics of sunlit and shaded leaves occur only if the direction of view coincides with or is near the direction of specular reflection. This is seen at those regions of the *Ficus* leaf in rows G and H of Fig. 22.7 where due to the appropriate local orientation of the curved leaf blade the sunlight is specularly reflected, the consequence of which is that in a considerable portion of these areas the leaf blade is overexposed due to the too intense reflected sunlight.

All these findings are in accord with the earlier results of Shul'gin and Moldau (1964), Vanderbilt and Grant (1985a,b), Vanderbilt et al. (1985a,b), Grant (1987), Grant et al. (1987a,b, 1993) and Sarto et al. (1989), who measured the polarized, non-polarized and specular reflectance of leaves of many different plant species as functions of the leaf surface features in the visible and near-infrared parts of the spectrum by point-source polarimetry. They found that in some viewing directions the surface reflection is so large that leaves appear white instead of green. In this case the strong specularly surface-reflected white light overwhelms the much smaller amount of green light scattered diffusely by the interior leaf tissue. They showed that the reflectance of the colourless and transparent leaf epidermis is practically independent of the wavelength of light, and in the visible part of the spectrum p of light reflected from green leaves is always the lowest in the green. They also demonstrated that the whitish light reflected specularly from leaves is always strongly polarized, while the green light reflected diffusely and non-specularly is practically unpolarized.

22.2.4 Do Polarization-Induced False Colours Influence the Weakly Polarization-Sensitive Colour Vision of *Papilio* Butterflies Under Natural Conditions?

Figures 22.3-22.6 and 22.8 clearly show that for the weakly polarization-sensitive model retina the polarization-induced false colours of plants fall near the real colours perceived by a polarization-blind retina even if they reflect strongly polarized light. Another effect of specular reflection is that whitish glare strongly masks the colour hue. Is the colour vision system of *Papilio* butterflies sensitive enough to perceive the tiny polarization-induced colour shifts in Figs. 22.3-22.6 and 22.8 under these circumstances? Behavioural studies on the discrimination of weakly saturated colours by insects are scarce. Honeybees seem to be able to discriminate pure white from white mixed with just a few percent of spectral light (Daumer 1963; Lieke 1984). Such stimuli differ in their locus position to a comparable degree as the loci of the real colours differ from some of the polarizational false colours calculated in this study. However, how well *Papilio* discriminates unsaturated colours remains to be demonstrated.

Horváth et al. (2002c) showed that in plant parts with dominating diffuse reflection, the colour saturation is relatively high but p is low. Although in this case hue discrimination will be good, the false colour effect is minute. On the other hand, plant surfaces with high p possess low colour saturation due to the white specularly reflected light. Thus, under natural conditions the weak polarization sensitivity of the photoreceptors might not interfere with the colour vision at all. This may be the reason why the average PS of the photoreceptors in proven colour-sensitive insects is not reduced to 1.0 but was found to be about 2.0-2.5 (*Cataglyphis bicolor*: Labhart 1986; *Papilio*: Kelber et al. 2001; *Drosophila melanogaster*: Speck and Labhart 2001; other fly species: Hardie 1985). Only in honeybees is the PS significantly smaller than 2 (Labhart 1980).

The complete destruction of the polarization sensitivity in a microvillar photoreceptor is not a trivial task but calls for a systematic misalignment of the microvilli along the rhabdom, in which complicated optical effects such as self-screening and lateral filtering within the rhabdom must be considered. The microvilli are misaligned by random or continuous direction changes (twist) along the rhabdom, but in most photoreceptors certain microvillar directions still dominate (Labhart and Meyer 1999). In honeybees, the rhabdom twists by about 180^{o} which reduces the *PS* to lower values than in other insects (Wehner et al. 1975; Labhart 1980). This might be taken as an indication that the exquisite colour vision system of honeybees might be more sensitive to small colour differences than that of other insect species and, thus, more compelled to avoid polarizational false colours.

Kelber (1999) and Kelber et al. (2001) showed that the colour choices of butterflies *Papilio aegeus* and *Papilio xuthus* is influenced by the E-vector orientation of linearly polarized light emitted by the colour stimuli to which the butterflies are exposed. They suggested that the interaction between colour and polarization might help the butterfly to find the best oviposition sites. Thus, they found that horizontally polarized green stimuli (mimicking horizontally oriented green leaves) were more attractive than vertically polarized stimuli of the same colour. At first glance, the findings of Kelber and collaborators, that polarization influences the colour choices of *Papilio* butterflies, seems to contradict the conclusion of Horváth et al. (2002c) that colour vision is quite insensitive to reflection polarization. However, in their behavioural tests, Kelber and collaborators used stimuli that had both a very high p ($\approx 100\%$) and a high degree of colour saturation, a situation that does not occur under natural conditions. Using this hyperstrong polarization/colour saturation combination, Kelber (1999) and Kelber et al. (2001) confirmed behaviorally the polarization sensitivity of *Papilio* photoreceptors that was previously measured electrophysiologically by Bandai et al. (1992). Thus, one can assume that this receptor property plays only a minor role in real life.

To demonstrate that the polarization sensitivity of the colour vision system can indeed ease certain vital tasks in a butterfly's life, further behavioural experiments with *Papilio* exposed to stimuli with natural combinations of p and colour saturation are needed. For an eye with $PS = 2$, even for almost totally polarized light reflected from a leaf of *Campsis radicans*, the false colour shifts in Fig. 22.6 should be smaller than those induced by the totally polarized and highly colour saturated stimuli of Kelber and co-workers, because the light reflected from leaves has rather low colour saturation. At the moment it is unknown how large a false colour shift needs to be in order to be just detectable, and thus useful in a behavioural context. Although Horváth et al. (2002c) did not claim that their calculations prove *Papilio* is incapable of detecting false colours under natural conditions, they did predict that the calculated colour shifts in the simulated *Papilio* retina may not large enough to be seen. The question, if *Papilio* might be equally sensitive to colours as bees and could perceive spectral shifts comparable to the calculated polarizational false colour shifts, can be answered only by further studies of the colour sensitivity of *Papilio*.

Another finding that seems to contradict the thesis of Horváth et al. (2002c) is that in plants the petals are usually less shiny than the leaves (Kay et al. 1981), i.e. specular reflection is reduced relative to diffuse reflection and, therefore, they exhibit less polarization. One might argue that this is to reduce false colour effects and, thus, to improve flower recognition. However, matter petals also avoid masking of the hue of a flower by whitish glare. The avoidance of glare alone may already be reason enough to reduce specular reflection in petals: the matter the petals, the more constant the appearence of flower colour when seen from different directions.

22.3 Polarizational False Colours Perceived by a Highly Polarization-Sensitive Retina Rotating in Front of Flowers and Leaves

It occurs frequently that insects hover in front of flowers and leaves, or approach the landing site on plant surfaces along oscillating flight paths, and their body axis more or less rotates to and fro simultaneously. Figures 22.9, 22.10, 22.11 and 22.12 demonstrate how the polarization-induced false colours perceived by a highly polarization-sensitive visual system (PS = 20) change in this situation. Figure 22.9 demonstrates well that the polarizational false colours of shiny leaves usually much more differ from their real colours than in the case of matt flower petals. The reason for this is that matt petals reflect light with lower p than shiny leaves. Rotating the head, the false colours of the leaves change more drastically than those of the petals: If the head's alignment χ with respect to the vertical changes from 0^o through 45^o and 90^o to 135^o, the false colours of the leaf in Fig. 22.9 change from violet through bluish and greenish to orange, while the false colours of the petals remain in the reddish-orange spectral range. There is no colour change in those regions of the flower where the reflected light is unpolarized. Here the colours perceived by the polarization-sensitive retina are the same as the real colours.

Figure 22.10 demonstrates how the polarization and the false colours induced by it change as a function of the orientation of the plant surface. In Fig. 22.10 the reflection-polarizational and spectral characteristics of green grass leaves in a meadow can be seen. The leaf blades are randomly oriented and curved, thus both p and α of reflected light change gradually from site to site. The consequence is that the real green colour of the grass becomes very heterogeneous resulting in practically all possible colour shades and hues ranging from violet through blue, yellow, orange to red. Thus, the originally relatively homogeneous green grass surface looks kaleidoscopic with randomly altering tiny false-coloured patches for a polarization-sensitive visual system, and what is more, the colours of the spots in this kaleidoscope change chaotically as the head rotates or the viewing direction alters.

Figure 22.11 shows the colours as well as the colours and brightness of *Epipremnum aureum*, the reflection-polarizational characteristics of which are

given in Fig. 22.4A, perceived by a polarization-blind ($P_R = P_B = P_G = 1$, β_R, β_G, β_B = arbitrary) and a highly polarization-sensitive ($P_R = P_B = P_G = 20$, $\beta_R = 0^o$, $\beta_G = 90^o$, $\beta_B = -45^o$) retina as a function of the alignment χ of the eye's dorso-ventral meridian with respect to the vertical. Here, both the shiny green leaves and the flower-imitating shiny red spathe reflect highly polarized light, induce striking false colours, the hues of which change drastically as the eye rotates in front of the plant.

If the eye regions viewing the flowers in flower visitors were polarization-sensitive, then colour-related behaviour, innate colour preferences, learned associations between nectar and flower colours, flower fidelity, colour constancy, chromaticity contrast between flowers and their background, nectar guides and other flower-pattern components, floral colour changes, true colour vision, or colour mimicry of flowers would lose their sense because of the disturbing effect of polarization-induced false colours. The consequence of these false colours would be that such flower visitors could not distinguish visually the flowers from other non-floral objects or the vegetable background.

22.4 Camouflage Breaking via Polarization-Induced False Colours and Reflection Polarization

We have seen above that generally polarization-induced false colours may be disadvantageous for perception of colour signals in the plant-pollinator interaction. However, Fig. 22.12A presents an example, when polarizational false colours could be advantageous in camouflage breaking for a predator. Figure 22.12A shows the colours as well as the colours and brightness of a beetle with shiny black carapace on a green leaf blade of *Helianthus annuus* perceived by a polarization-blind ($P_R = P_B = P_G = 1$, β_R, β_G, β_B = arbitrary) and a highly polarization-sensitive ($P_R = P_B = P_G = 20$, $\beta_R = 0^o$, $\beta_G = 90^o$, $\beta_B = -45^o$) retina as a function of the alignment χ of the eye's dorso-ventral meridian with respect to the vertical. The recording was taken under a clear sky, the scene was illuminated by direct sunlight and the originally colourless carapace of the beetle reflected green light from the surrounding vegetation and blue light from the sky. Thus, the carapace has a greenish-bluish appearance, which reduces the colour contrast between the beetle and the green leaf. This effect results in a moderate colour camouflage of the carapace for a polarization-blind visual system. However, this camouflage is broken for a highly polarization-sensitive visual system perceiving the striking polarizational false colours of the carapace, which differ considerably from those of the leaf blade. The polarization-induced false colours change dramatically as the eye rotates, which further enhances the break of the colour camouflage.

Figure 22.12B shows the patterns of p and α of the beetle and the underlying leaf measured by video polarimetry in the green (550 nm), which patterns are practically the same also in the red (650 nm) and blue (450 nm). We can see that

there is also a remarkable p- and α-contrast between the carapace and the leaf blade, because the horizontal and slightly rough surface of the leaf reflects horizontally polarized light with relatively low p, while the strongly curved and smooth carapace reflects highly polarized light with spatially changing α. Hence, break of the camouflage of the carapace occurs not only for a highly polarization-sensitive colour vision system, but also for a visual system with true polarization vision, which is able to perceive the large p- and α–contrasts between the beetle and the substratum.

Camouflage breaking via polarization-induced false colours or reflection-polarization is a possible visual phenomenon, which would be worth testing in the future. The possible breaking of the brightness and colour camouflage of hidden animals (e.g. caterpillars or frogs on leaves) by means of reflection polarization was suggested by Shashar et al. (1995a).

22.5 Is Colour Perception or Polarization Sensitivity the more Ancient?

Honeybees need accurate colour vision in order to find properly the flowers to gather nectar and pollen. They also need polarization sensitivity (PS) to orient by means of the celestial polarization pattern. The perception of polarization is ensured by the dorsal rim area (DRA) of the compound eye, where monochromatic and highly polarization-sensitive photoreceptors are gathered. Horváth and Varjú (2003) proposed that the polarization-sensitive receptors with non-twisted microvilli in the DRA and the polarization-insensitive receptors with twisted microvilli in other eye regions of honeybees and many other insects support the hypothesis that perception of polarization is a more ancient visual capability than perception of colours.

We have seen above that unambiguous colour vision can be ensured only by means of polarization-insensitive photoreceptors. In a compound eye composed of photoreceptors with microvilli such polarization insensitivity can be ensured by a random orientation of the microvilli. Morphologically, this would be the simplest and easiest way to abolish the inherent PS of the microvilli. Using exclusively such polarization-blind photoreceptors, bees could precisely discriminate the colours and find the adequate flowers in a meadow, but they could not find the way backwards to their nest if the sun is occluded by clouds. The latter would be lethal for them.

Contrary to this, however, if the non-twisted photoreceptors were polarization sensitive due to the parallel orientation of the microvilli in the entire eye, bees could orient by means of the celestial polarization even if the sun is not visible, and could navigate back to their nest. The cost of this would be, that the colour perception would be ambiguous because of the polarization-induced false colours. Although in this case bees could not find easily the proper flowers on the basis of their characteristic colour patterns, this imperfection could be partly compensated by using other sensory cues, such as the characteristic shape or odour of flowers.

Although polarization-sensitive compound eyes could be frequently deceived by the polarizational false colours, the resulting wrong landing on plant leaves or inappropriate flowers instead of landing on the sought flower petals with given colours would not be deadly. This would only decrease more or less the efficiency of nectar and pollen gathering in bees. On the basis of the above we propose the following evolutionary scenario:

1. In the compound eyes of the ancestors of bees polarization-sensitive, non-twisted photoreceptors with parallel microvilli evolved in the whole eye in order to orient by means of the celestial polarization pattern.
2. Since the absorption spectrum of photopigments is relatively narrow, receptors with different spectral sensitivities were needed to perceive the near-UV and visible ranges of the spectrum. Thus, UV-, blue- and green-sensitive receptors evolved in the ancestors of bees.
3. In a later stage of evolution, apart from the DRA of the eye, the polarization-induced false colours of plant surfaces were eliminated by the proper twist of photoreceptors. Polarization-sensitivity remained only in the DRA of the eye, where polarizational false colours do not cause any problem, because here only UV receptors occur.

The regular twist of the photoreceptors in bee eyes may hint that polarization sensitivity is more ancient than colour perception. Polarization-sensitive receptors need only to be twisted in order to abolish their inherent polarization sensitivity. Would the colour perception be the more ancient, the microvilli of ancient photoreceptors would have originally been randomly oriented to ensure polarization-blindness and unambiguous colour discrimination. Later, polarization-sensitive receptors with parallel microvilli should have been gradually evolved from such receptors, if the ancestors of bees could have survived the lack of the capability of orientation by means of celestial polarization.

The above proposal is consistent with the findings of Chittka (1996) that the essential components of bee's colour vision predated the evolution of flower colour, because the spectral receptor sets of bees are indistinguishable from those of many members of arthropod taxa, whose evolutionary lineages diverge from those of bees before there were flowers. The Cambrian ancestors of extant insects and crustaceans possessed already UV, blue and green receptors. Insects were well preadapted for flower colour coding more than 500 million years ago, about 400 million years before the extensive radiation of the angiosperm plants which started in the middle Cretaceous (100 million years ago), although the origin of the angiosperms might have to be placed in the Triassic. According to Chittka (1996), flower colours had no impact on wavelength positioning of bee photoreceptors. In contrary, because bee colour vision is optimally suited to code flower colour, flower colours should adapted to insect vision.

Table

Table 22.1. Intensity I, degree of linear polarization p and angle of polarization α (measured from the vertical) of a pixel of a leaf in Fig. 22.2 measured by video polarimetry at 650 nm (R), 550 nm (G) and 450 nm (B). The data in rows 1-3 are used in the calculations of Fig. 22.5. Using the original degrees of polarization p_0 in row 3, the other degrees of polarization are derived as follows: $p_i = n_i \cdot p_0$, i = 1,2,...,8. These data are used in the calculations of Fig. 22.6. (After Table 2 of Horváth et al. 2002c, p. 3290).

row		**R**	**G**	**B**
1	I (%)	78	87	100
2	α	105°	107°	108°
3	$p_0(R,G,B)$ (%)	61	59	78
	$p_i(R,G,B) = n_i \cdot p_0(R,G,B)$ (%)			
4	$n_1 = 0$	0	0	0
5	$n_2 = 0.18$	11	10	14
6	$n_3 = 0.36$	22	21	28
7	$n_4 = 0.55$	33	32	42
8	$n_5 = 0.73$	44	43	57
9	$n_6 = 0.91$	55	53	71
10	$n_7 = 1.09$	66	64	85
11	$n_8 = 1.28$	78	75	99

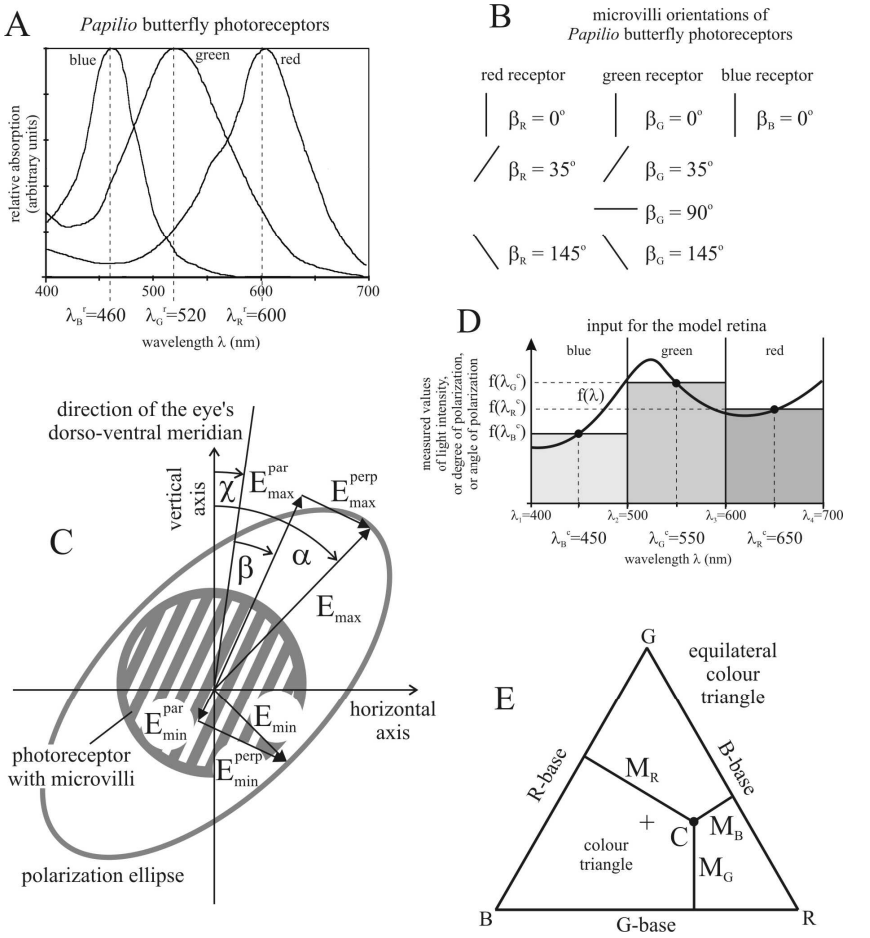

Fig. 22.1. A: Relative absorption functions of the blue, green and red photoreceptors of *Papilio xuthus*. B: Microvilli orientations β measured clockwise from the eye's dorso-ventral meridian in the photoreceptors of different spectral types in *Papilio xuthus*. C: Definition of the different parameters of partially linearly polarized light and a polarization-sensitive photoreceptor. The direction of hatching indicates the microvilli orientation β. The angle of the eye's dorso-ventral meridian is χ clockwise from the vertical. α is the angle of polarization of light measured clockwise from the vertical. The arrows represent the maximum (E_{max}) and minimum (E_{min}) of the electric field vector (the major and minor axes of the polarization ellipse) and their components that are parallel (E^{par}_{min}, E^{par}_{max}) or perpendicular (E^{perp}_{min}, E^{perp}_{max}) to the microvilli. D: Replacement of the blue (400–500 nm), green (500–600 nm) and red (600–700 nm) parts of function $f(\lambda)$ [$f = I$ (intensity), or $f = p$ (degree of linear polarization), or $f = \alpha$ (angle of polarization)] by discrete constant values $f(\lambda_r^c)$ $(r=B,G,R)$ measured by video polarimetry at wavelengths λ_r^c. E: Position of a visual stimulus C with spectral components M_R, M_G and M_B within the equilateral colour triangle of a colour-sensitive visual system with photoreceptor types R, G and B. The centre of the triangle is marked by +. (After Fig. 1 of Horváth et al. 2002c, p. 3283).

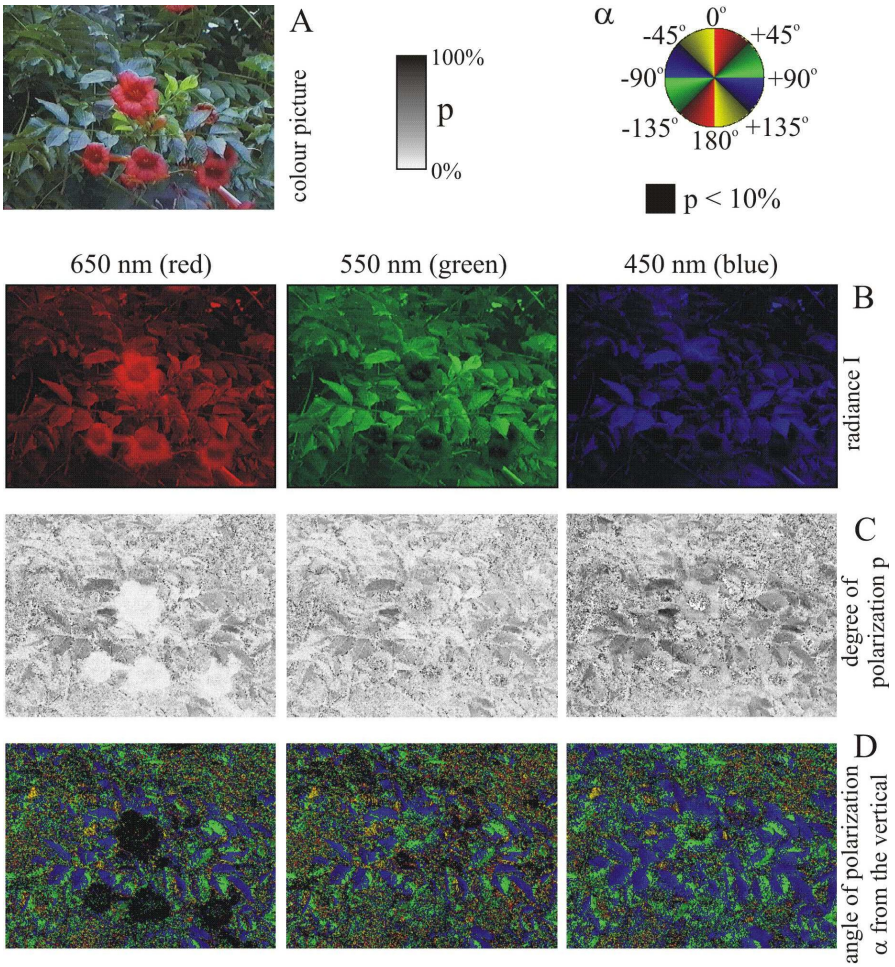

Fig. 22.2. A: Colour picture of red flowers and green leaves of *Campsis radicans* (trumpet vine, Bigniniaceae). B-D: Patterns of radiance I, degree of linear polarization p and angle of polarization α (measured from the vertical) of the plant surfaces in A measured by video polarimetry at 650, 550 and 450 nm. Number of pixels = 560×736 = 412160. In row C regions are black where $p < 10\%$. (After Fig. 3 of Horváth et al. 2002c, p. 3286).

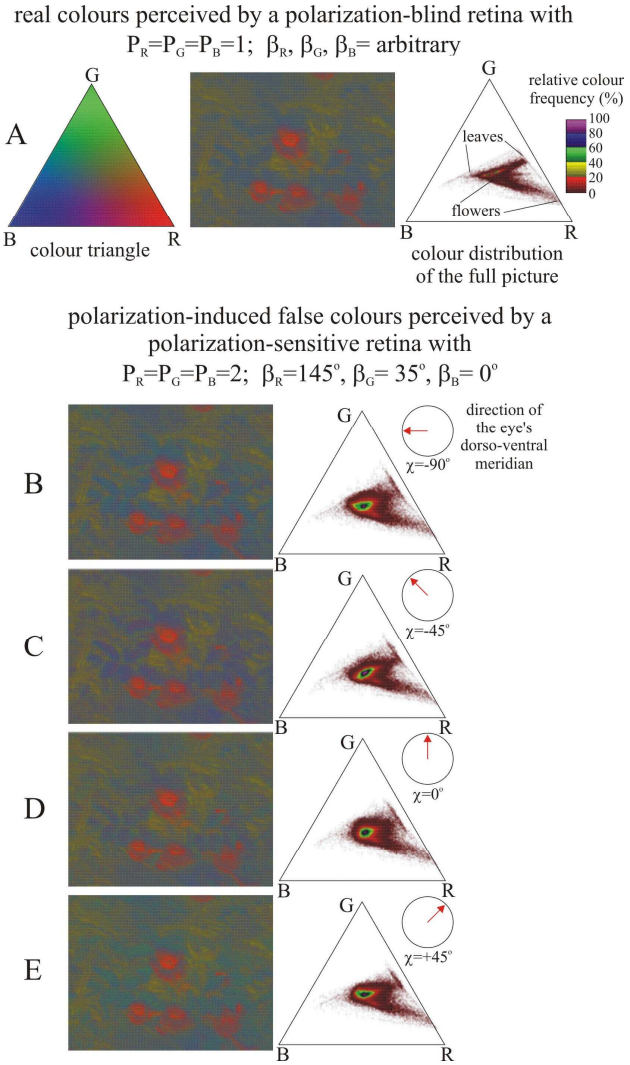

Fig. 22.3. A: Left: Equilateral R-G-B colour triangle filled with the isoluminant colour shades used. Middle: Real colours of *Campsis radicans* in Fig. 22.2A as perceived by a polarization-blind retina with polarization sensitivity $P_R = P_G = P_B = 1$ and microvillar directions β_R, β_G, β_B = arbitrary. Right: Relative frequency distribution of perceived colours (M_R, M_G, M_B) within the colour triangle calculated for the full rectangular picture. B-E: Polarization-induced false colours of *C. radicans* perceived by a polarization-sensitive retina with $P_R = P_G = P_B = 2$, $\beta_R = 145^\circ$, $\beta_G = 35^\circ$, $\beta_B = 0^\circ$ and their relative frequency distribution in the colour triangle as a function of the alignment χ of the eye's dorso-ventral symmetry plane (indicated by red arrows in the circular insets) measured from the vertical. Note that the isoluminant rectangular images and the isoluminant colour triangle on the left in row A give information on colour alone; intensity information is missing. (After Fig. 4 of Horváth et al. 2002c, p. 3288).

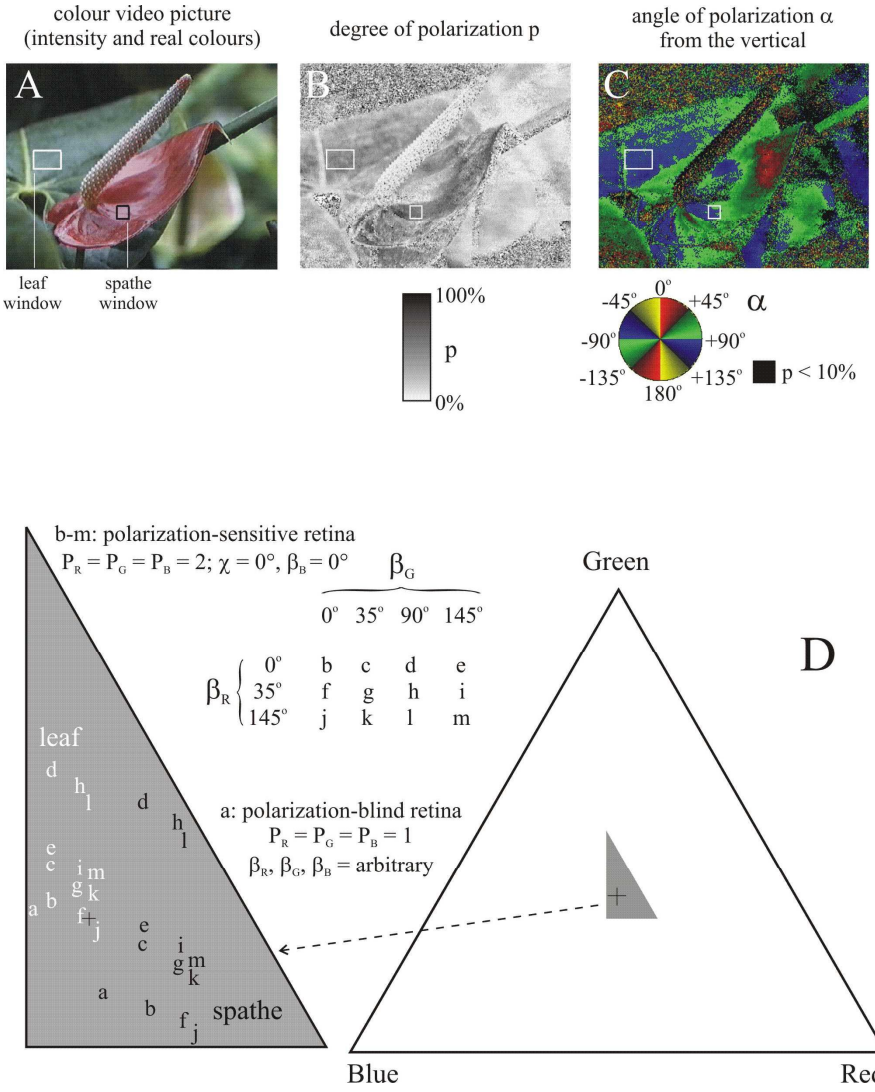

Fig. 22.4. A-C: Colour picture and patterns of the degree p and angle α of linear polarization of *Epipremnum aureum* (golden pothos, Aracea) measured by video polarimetry at 450 nm. D: Colours (M_R, M_G, M_B) of *E. aureum* perceived by a polarization-blind retina with $P_B = P_G = P_R = 1$, and β_R, β_G, β_B = arbitrary (*a*), and by a polarization-sensitive retina with $P_B = P_G = P_R = 2$, $\chi = 0^o$, $\beta_B = 0^o$ as a function of the microvillar directions β_G and β_R of the green and red receptors (*b-m*). Every microvilli situation is designated by a lower case letter ranging from *a* to *m*. The corresponding spectral loci (designated by letters *a-m*) of two details of the picture, one on a leaf blade (white) and one on the spathe (black) marked by rectangular windows in patterns A-C, are plotted within the equilateral R-G-B colour triangle, the colourless centre of which is represented by +. (After Fig. 6 of Horváth et al. 2002c, p. 3291).

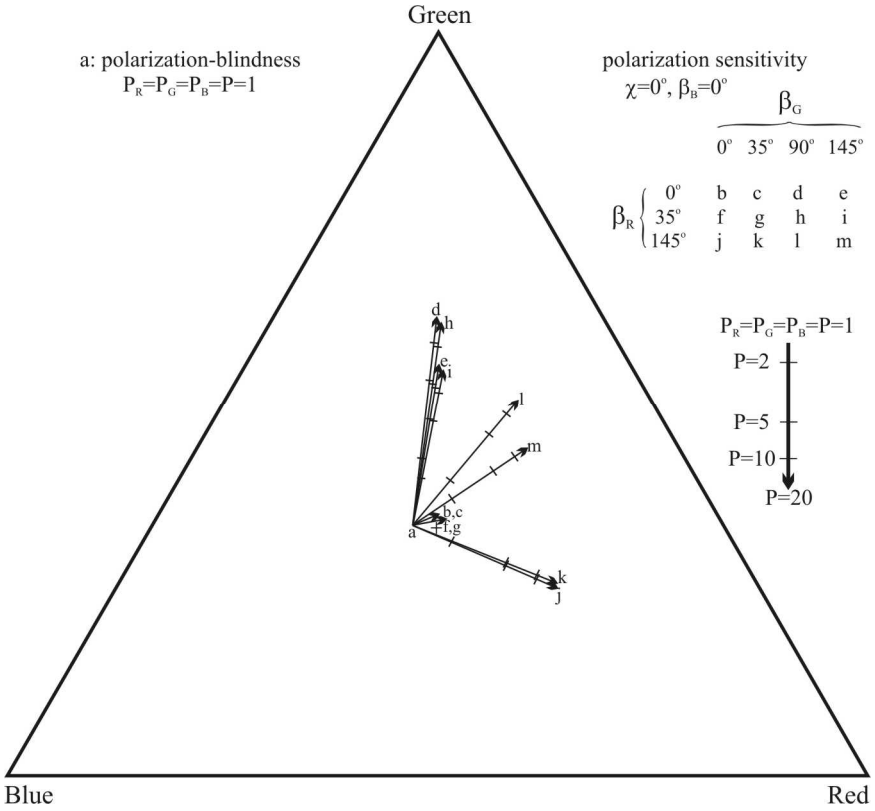

Fig. 22.5. Dependence of the polarization-induced false colour (M_R, M_G, M_B) perceived by a retina with $\chi = 0^o$, $\beta_B = 0^o$ on the polarization sensitivity $P_B = P_G = P_R = P$ as a function of the microvillar directions β_G and β_R of the green and red receptors (designated by lower case letters *b*-*m*) plotted within the equilateral R-G-B colour triangle, the colourless centre of which is represented by +. The colours are calculated for a point on a leaf of *Campsis radicans*, the reflection-polarizational characteristics of which are given in Table 22.1. The arrows start from the spectral locus *a* of the real colour when $P_B = P_G = P_R = P = 1$, meaning polarization-blindness, while the arrowheads point to the spectral locus of perceived false colours if $P_B = P_G = P_R = P = 20$. The spectral loci of false colours for P ranging between 1 and 20 are placed along the straight arrows, on which the loci for $P = 2$, 5 and 10 are marked by bars. (After Fig. 7 of Horváth et al. 2002c, p. 3292).

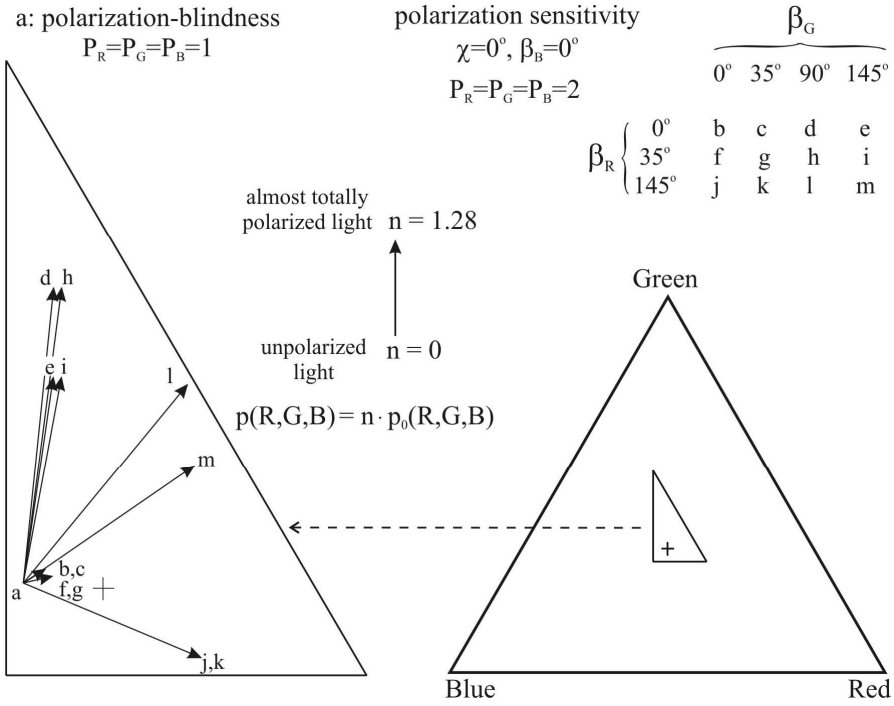

Fig. 22.6. Dependence of the polarization-induced false colour (M_R, M_G, M_B) perceived by a polarization-sensitive retina with $P_B = P_G = P_R = 2$, $\chi = 0^o$, $\beta_B = 0^o$ on the degree of linear polarization $p(R,G,B)$ of reflected light as a function of the microvillar directions β_G and β_R of the green and red receptors (designated by lower case letters *b*-*m*) plotted within the equilateral R-G-B colour triangle, the colourless centre of which is represented by +. The colours are calculated for the point of a leaf of *Campsis radicans*, the original reflection-polarizational characteristics of which are given in Table 22.1. The degrees of linear polarization of reflected light are calculated as $p(R,G,B) = n \cdot p_0(R,G,B)$ and given in Table 22.1, where n is an arbitrary factor. The arrows start from the spectral locus *a* of the real colour when $n = 0$ (unpolarized light) and $P_B = P_G = P_R = P = 1$ (polarization-blindness), while the arrowheads point to the spectral locus of perceived false colours for $n = 1.28$ (almost totally polarized light in all three spectral ranges). The spectral loci of false colours for n ranging between 0 and 1.28 are placed approximately equidistant along the straight arrows. (After Fig. 8 of Horváth et al. 2002c, p. 3293).

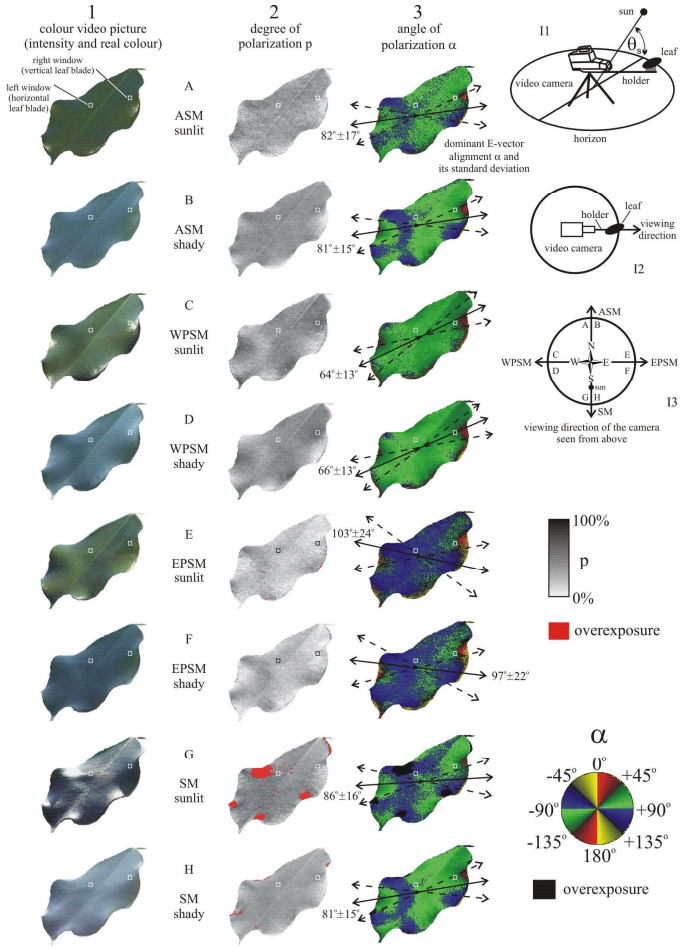

Fig. 22.7. Spectral and reflection-polarizational characteristics of a leaf of a *Ficus benjamina* tree (weeping fig, Ficaceae) as functions of the illumination conditions in the open. The leaf was mounted in front of the camera on a horizontal rod, which rotated in a horizontal plane along a vertical axis together with the camera (insets I1 and I2). The solar elevation was $\theta_S = 55^o$ and the leaf was illuminated by direct sunlight (A,C,E,G) or shaded with a small screen (B,D,F,H) which just occluded the sun and exposed the leaf to the full clear sky. In the small rectangular left and right window, the leaf blade is approximately horizontal and vertical, respectively. Inset I3 shows the four different horizontal directions of view of the camera with respect to the solar azimuth. ASM: antisolar meridian, SM: solar meridian, EPSM: eastwardly perpendicular to the solar meridian, WPSM: westwardly perpendicular to the solar meridian. *Column 1*: Colour pictures of the leaf. *Column 2*: Patterns of the degree of linear polarization p of the leaf measured by video polarimetry at 450 nm. *Column 3*: Patterns of the angle of polarization α (measured from the vertical) of the leaf at 450 nm, where the dominant (average) E-vector alignment of the leaf blade is represented by a double-headed solid arrow, while the standard deviations are shown by double-headed dashed arrows. (After Fig. 9 of Horváth et al. 2002c, p. 3294).

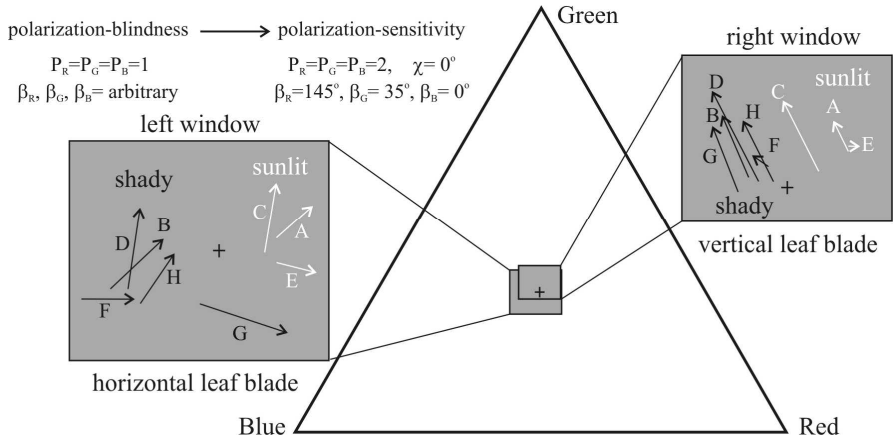

Fig. 22.8. Spectral loci (designated by capitals A-H, representing the situations A-H in Fig. 22.7) of the leaf areas marked with a left and a right small rectangular window in Fig. 22.7 plotted within the equilateral R-G-B colour triangle, the colourless centre of which is represented by +. The arrows start from the spectral locus of real colours perceived by a polarization-blind retina with $P_B = P_G = P_R = 1$ and β_R, β_G, β_B = arbitrary, while the arrowheads point to the spectral locus of false colours perceived by a polarization-sensitive retina with $P_B = P_G = P_R = 2$, $\chi = 0^o$, $\beta_R = 145^o$, $\beta_G = 35^o$, $\beta_B = 0^o$. (After Fig. 10 of Horváth et al. 2002c, p. 3295).

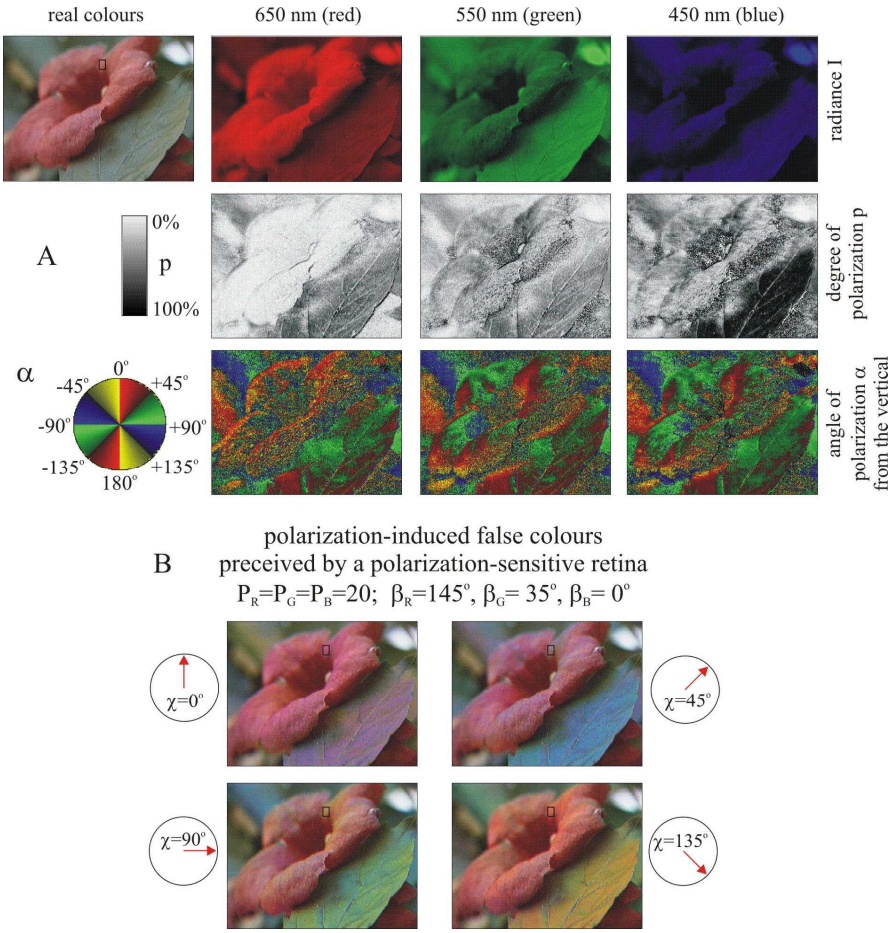

Fig. 22.9. A: Reflection-polarizational characteristics of a reddish flower and a green leaf of *Campsis radicans* measured by video polarimetry in the red, green and blue. B: Brightness and polarization-induced false colours of the same plant perceived by a highly polarization-sensitive retina with $P_R = P_B = P_G = 20$, $\beta_R = 0^o$, $\beta_G = 90^o$, $\beta_B = -45^o$ as a function of the alignment χ of the eye's dorso-ventral meridian with respect to the vertical. In the circular insets the red arrow shows the actual value of χ.

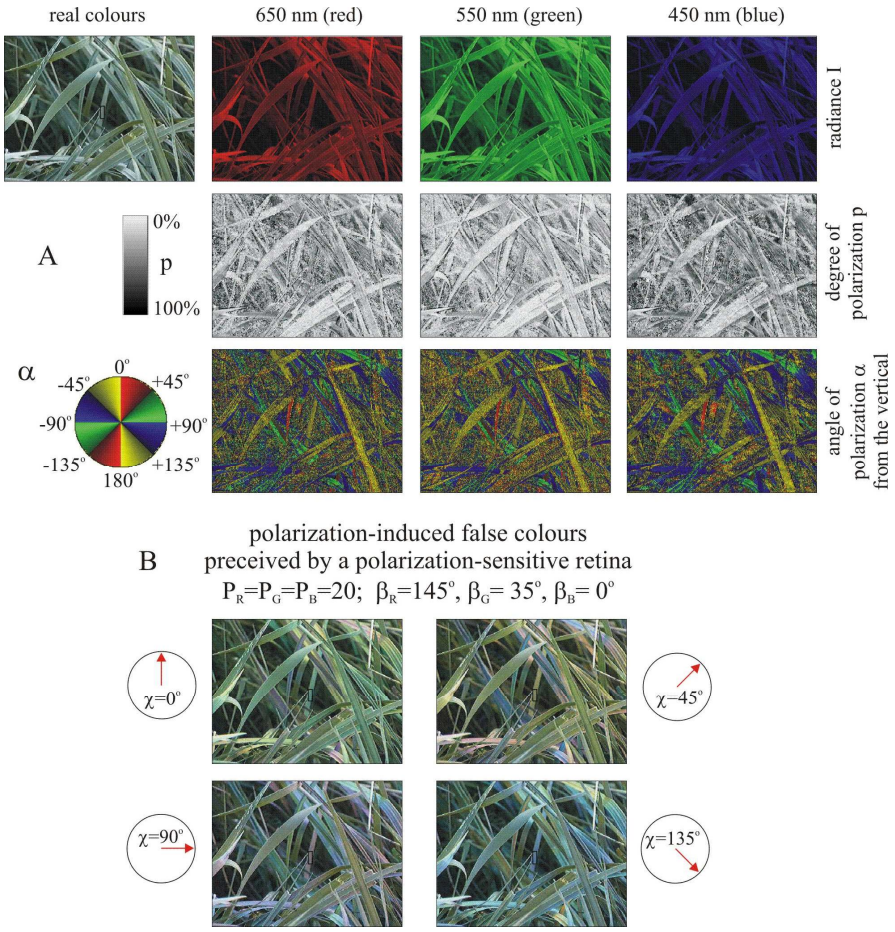

Fig. 22.10. As Fig. 22.9 for shiny green grass leaves in a meadow.

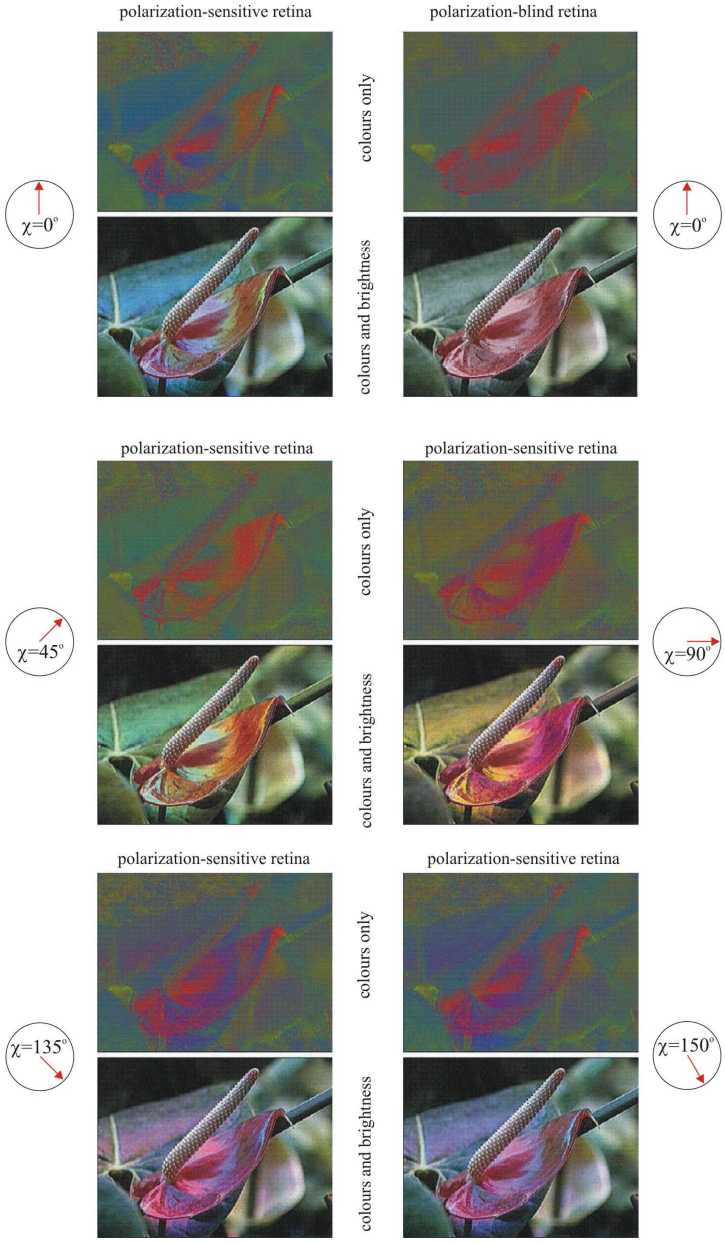

Fig. 22.11. Colours as well as colours and brightness of *Epipremnum aureum* perceived by a polarization-blind ($P_R = P_B = P_G = 1$, β_R, β_G, β_B = arbitrary) and a highly polarization-sensitive ($P_R = P_B = P_G = 20$, $\beta_R = 0^o$, $\beta_G = 90^o$, $\beta_B = -45^o$) retina as a function of the alignment χ of the eye's dorso-ventral meridian with respect to the vertical. In the circular insets the red arrow shows the actual value of χ.

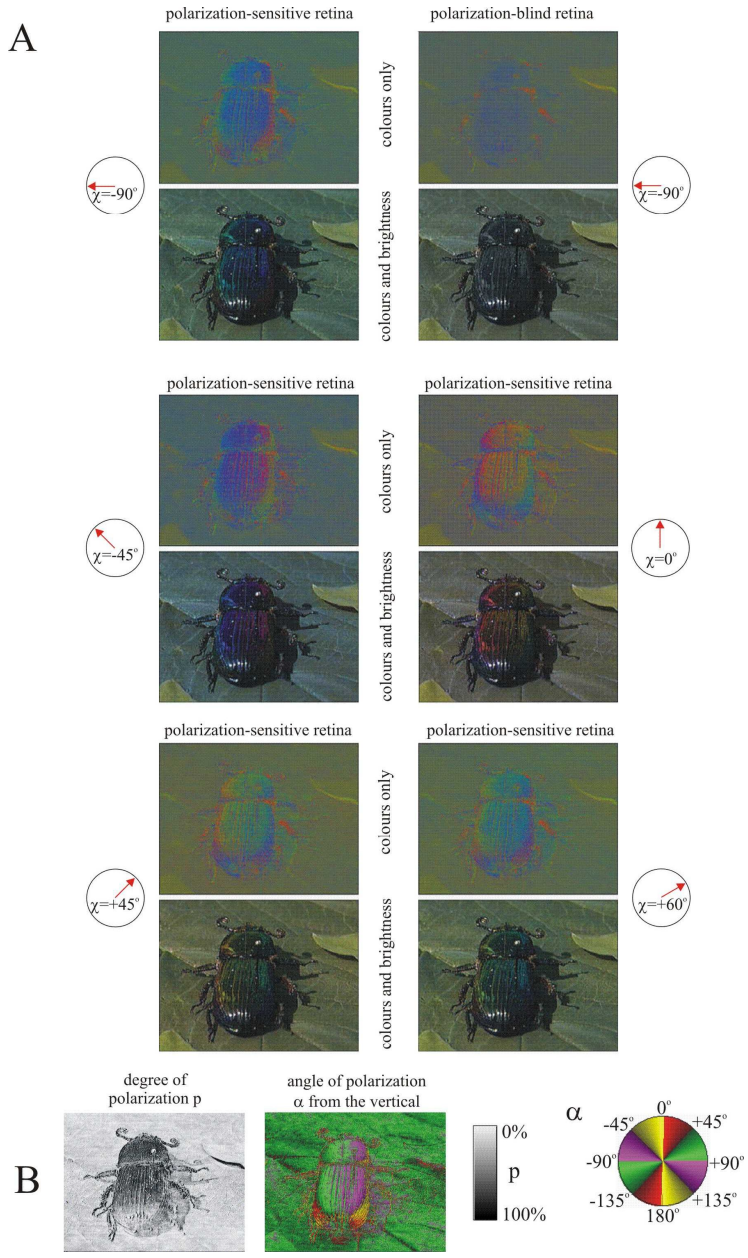

Fig. 22.12. A: As Fig. 22.11 for a beetle with shiny black carapace on a green leaf blade of *Helianthus annuus*. The recording was taken under a clear sky. The scene is illuminated by direct sunlight and the originally colourless (shiny black) carapace of the beetle reflects blue skylight and green light from the surrounding vegetation. B: Patterns of the degree p and angle α of linear polarization of the scene measured by video polarimetry at 550 nm.